Effect of admixture on the pore structure refinement and enhanced performance of alkali-activated fly ash-slag concrete

Keulen, A.; Yu, Q. L.; Zhang, S.; Grünewald, S.

DOI
10.1016/j.conbuildmat.2017.11.136

Publication date
2018

Document Version
Accepted author manuscript

Published in
Construction and Building Materials

Citation (APA)
Keulen, A., Yu, Q. L., Zhang, S., & Grünewald, S. (2018). Effect of admixture on the pore structure refinement and enhanced performance of alkali-activated fly ash-slag concrete. *Construction and Building Materials*, *162*, 27-36. https://doi.org/10.1016/j.conbuildmat.2017.11.136

Effect of admixture on the pore structure refinement and enhanced performance of alkali-activated fly ash-slag concrete

A. Keulen [1,2,*], Q.L. Yu [1,*], S. Zhang [3], S. Grünewald [3,4]

[1] Eindhoven University of Technology
Department of the Built Environment
P.O. Box 513, 5600 MB Eindhoven
The Netherlands
Tel: +31 (0)40 247 2371
Fax: +31 (0)40 243 8595
Email: g.yu@bwk.tue.nl

[2] Van Gansewinkel Minerals
Eindhoven, The Netherlands
E-mail: arno.keulen@vangansewinkel.com

[3] Delft University of Technology
Faculty of Civil Engineering and Geosciences
Delft, The Netherlands

[4] CRH Sustainable Concrete Centre
Oosterhout, The Netherlands

(*) to whom correspondence should be addressed

Abstract

This paper investigates the influence of a plasticizing admixture on the pore structure refinement of alkali-activated concrete and paste mixtures and the consequently enhanced performance. Alkali-activated fly ash-slag concrete and paste are designed using a polycarboxylate-based admixture with different dosages. The pore structure and porosity are analyzed using mercury intrusion porosimetry (MIP). The workability, compressive strength, chloride migration resistance and electrical resistivity of alkali-activated fly ash-slag concrete and paste are determined. The results show that significantly improved workability and strength development are obtained at an increased admixture content. The admixture improves the gel polymerization product layer most likely around the GGBS particles, densifying the matrix. The 28-day Cl-migration coefficient of admixture (1-2 kg/m^3) modified concrete is equal to the reference mixture, while at the highest admixture content the Cl-ingress is increased. At the later ages (91- days), the Cl-migration coefficients of all concretes, non- and admixture-containing samples, are comparable and low (about 2.6×10^{-12} m^2/s). The MIP analyses show a significant decrease of the total and effective capillary porosity over time at an increased admixture content. The relationships between the porosity and other properties are discussed, at varying admixture contents.

Keywords: alkali activated fly ash-slag concrete, admixture, workability, microstructure, compressive strength, chloride migration, pore structure

1 Introduction

Alkali activated slag/ fly ash based binders in comparison with traditional Portland cement possess comparable to moderately modified material properties (i.e. mechanical strength, chloride ingress, acid and carbonation resistance) [1–4]. Designing alkali activated materials (AAM) with high durability performance largely depends on the mixture composition (design). This is mainly controlled by the applied precursor minerals such as ground granulated blast furnace slag (GGBS) and pulverized coal fly ash (PCFA), and the concentration, type and combination of alkaline activators (i.e. sodium or potassium silicate or hydroxide). More specifically, a higher GGBS content (0 to 100 wt.%) as a replacement of the PCFA in the binder, favors the matrix densification and strength development [5–8]. By forming mainly calcium dominated gel- structures (C-A-S-H), consequently resulting in a reduced chloride migration rate in concrete [9]. However, to support the practical application and further development of AAM as well as that of Portland cement, both materials are strongly dependent on the availability of admixtures [10,11]. Due to the existence of multiple molecular varieties, admixtures (known as superplasticizers (SP's)) can perform very differently in optimizing the fresh concrete mixture state, although this is also dependent on the binder type and composition [12].

For fly ash dominated AAM systems, the mixture workability, setting time and liquid demand can be relatively easily modified by polycarboxylate and naphthalene type admixtures [13–17]. Although often relatively high admixture dosages (≥ 1-10 wt.% in relation to the binder content) are required in order to gain a high mixture flowability and consistency [15,17–19], compared to that of Portland cement mixtures (mostly ≤ 1 wt.%). As a consequence, high dosages lead to unwanted negative side effects, such as increased material porosity and loss of mechanical strength [15,17]. For GGBS-dominated AAM, almost all related admixtures often do not sufficiently modify the mixture workability [20]. In some cases, mixture rheology improvement and setting time retardation are observed to a certain extent when using only a hydroxide instead of a silicate based activator [15,20]. Overall, many of these studies indicate that admixtures are able to reduce the liquid to binder ratio or liquid demand of the fresh mixture.

Summarizing relevant literature dealing with the effect of mainly Portland cement based admixtures on AAM systems, the following remarks can be drawn:

- Admixtures shows no improvement to the delay of the mixture setting time and overall mixture workability, which could be associated with their physical and chemical incompatibility or rapid chemical oxidation in the high alkali system [13,15,20].
- Admixtures mainly enhance the AAM mixture workability over a short period of time (≤ 10-40 min). An increasing GGBS and silicate activator content strongly reduce the workability, therefore AAM is often prone to a non-predictable, very rapid decline of the workability and fast setting [15,16,18,20–22].
- Naphthalene and polycarboxylate admixtures are the most effective SPs, to enhance the mixture workability of mainly alkali activated PCFA systems [13,15,16] compared to GGBS based systems [15,18,22,23].
- Admixtures use frequently causes negative effects on the setting time and mechanical property of AAM [13,15–18,20–22,24].
- Admixtures can have either negative or positive effects on the concrete shrinkage [20,24].

Limited experimental studies have been performed on the effect of admixtures on AAM systems as often admixtures are not able to sufficiently modify AAM concrete [20,25]. However, in recent years, more, while still rather limited commercial admixtures, mainly polycarboxylates, are available for AAM. Further knowledge is required in order to improve the physical and chemical understanding of their working mechanisms, as well as that of their predictability with AAM concrete production.

Apart from the rheology modifying ability [14], another positive effect is that the microstructure development of AAM concrete can be significantly enhanced by a polycarboxylate. Through densification of the interfacial transition zone (ITZ) [26], located between the newly formed AAM gel structure and solid particles (binder and the aggregate minerals), at which the porosity is reduced. This leads to the shift of pore size of hardened AAM towards smaller ranges which improves the material performance by for instance a higher material strength, reduced permeability and enhanced ion diffusion resistance (e.g. chloride).

104 However, the microstructure development (i.e. porosity and permeability) and the chloride
105 migration of AAM concrete under the influence of using admixture have not been studied.
106 Research is needed to understand the potential physical and chemical mechanisms affected by
107 a working admixture in concrete, contributing to the design of durable AAM concretes for
108 construction structures.
109 In the present study, a comprehensive approach is applied to investigate the effect of
110 admixture on pore structure refinement and enhanced performance of alkali-activated fly ash-
111 slag concrete. The main objectives of this study are:
112 • Analyze the influence of the admixture content on the fresh mixture state properties, by
113 measuring the setting time and the workability progression over time;
114 • Study the influence of the admixture content on the hardened material state properties, by
115 analyzing the AAM compressive strength, chloride migration rate and material electrical
116 resistivity over time;
117 • Determine the effect of admixture content on the AAM pore structure and progression
118 over time and consequent influence on the material durability (chloride migration);
119 • Investigate the relation between different system parameters and their significance; such
120 as concrete compressive strength and porosity and their effect on the permeability and
121 chloride migration of concrete over time under the influence of the admixture content.
122
123
124

2 Experimental setup

2.1 Materials

The used mineral binder (MB) is a blend of 73.7 wt.% pulverized coal fly ash (PCFA) class F in accordance with NEN-EN 450 with 25 wt.% granulated ground blast furnace slag (GGBS) and 1.3 wt.% technical grade sodium meta-silicate pentahydrate powder (supplied by PQ, The Netherlands). The elemental composition of the MB is determined by X-ray fluorescence (XRF), as shown in Table 1.

Table 1: Elemental composition (%) of the mineral binder (MB), determined with XRF.

Oxides	PCFA	GGBS	MB
SiO_2	59.7	34.3	51.4
Al_2O_3	24.6	9.8	17.9
CaO	1.5	41.8	13.9
Fe_2O_3	6.8	0.5	6.3
MgO	1.3	7.7	3.8
K_2O	3.0	0.6	2.2
Na_2O	0.6	<0.1	1.1
TiO_2	1.2	1.2	1.1
Mn_3O_4	0.0	0.3	0.2
BaO	0.1	0.1	0.1
P_2O_5	0.1	<0.1	0.4
SO_3	1.0	3.6	1.7
Cl	<0.1	<0.1	<0.1
LOI (950 °C)	0.9		1.6

LOI: loss of ignition

River aggregates (sand 0-4 mm and gravel 4-16 mm) were used to produce the mixtures. A commercial 33% liquid sodium hydroxide (NaOH) with a molarity (M) of 11.2 was diluted by tap water to obtain the desired (3M NaOH) system alkalinity. A polycarboxylate plasticizing admixture (supplied by SQAPE Technology), hereafter identified as “admixture”, was used to enhance the fresh concrete workability. The polycarboxylate is highly soluble in water and the

backbone contains poly-functional reactive side chains, e.g. carboxyl, which initiate the metal (mainly calcium) adsorption reactions. Preliminary research shows that a chemical oxidation effect is observed when mixing this admixture with NaOH solution that helps to improve the workability. The added additional water, NaOH and the admixture were summed as the total liquid volume (although solids are present). The relevant material properties, including the specific density, water absorption and mean particle size (d_{50}), are listed in Table 2.

Table 2: Materials characteristics.

Material	Density (kg/m^3)	Water Absorption (%)	d_{50} (μm)
PCFA	2312		20
GGBS	2893		12
Mineral binder (MB)	2498		15
Sand (0-4 mm)	2600	0.80	
Gravel (4-16 mm)	2590	1.80	
Meta silicate powder	900		650 till 900
NaOH solution (33 % pure)	1360		
Admixture	1190		

* PSD: particle size distribution

2.2 Binder composition and admixture

A predefined AAM binder was used in this study, composing of: (1) the blended mineral binder with meta-silicate and (2) a fixed 3 M NaOH activator. Preliminary research and the literature [27] verified that this relatively low activator molarity is able to effectively promote an acceptable setting time and sufficient mechanical strength performance of AAM concrete. The low silicate powder addition, as a part of the MB, is applied to increases the material strength at the early ages of 1 day to 7 days, while higher silicate dosages (> 1.3 wt.%) would reduce the mixture workability. Additionally, the plasticizing and liquid reducing effects of the admixture on paste mixtures containing sole PCFA or GGBS were examined by performing the water demand experiments [28]. The results showed that a significant decrease of liquid demand up to 25 % for both PCFA and GGBS can be observed. In overall, PCFA shows a lower liquid demand

with an overall factor of about 2 of GGBS. Based on the preliminary study, a high PCFA content (≈ 75 wt.%) was used for the mineral binder composition, concerning both the mixture liquid demand and binder performance.

2.3 Sample preparation

2.3.1 Concrete mixtures

The concrete mixtures (Table 3) were analyzed on workability (slump) and tested on the compressive strength, the chloride migration rate and the material electrical resistivity over time, to evaluate the effect of admixture. The mixtures (140 L per batch) were prepared with a high-speed rotating pan mixer. During the mixture preparation, firstly sand, gravel and the solid precursors were mixed and then the liquid was added. The total mixing time was 5 min: 1 min of dry mixing (sand, gravel with solid precursors) and 4 min of additional mixing (adding the total liquid). Fresh concrete was cast in steel molds (150 × 150 × 150 mm^3), finished on a compaction table and sealed with a plastic foil. After 24 hours of room temperature curing, the specimens were demolded, covered by plastic and stored at room temperature (≈ 20 °C).

Table 3: Mixture composition of AAM concretes.

Mixture code	Sand (wt.%)	Gravel (wt.%)	Binder (kg/m^3)	Total liquid (l/m^3)	L/B ratio	NaOH (M)	Admixture (kg/m^3)
A	47	53	400	127	0.32	3	0.0
B	47	53	400	127	0.32	3	1.0
C	47	53	400	127	0.32	3	2.0
D	47	53	400	127	0.32	3	3.0
E	47	53	400	127	0.32	3	4.0
F	47	53	400	127	0.32	3	5.0

2.3.2 Paste mixtures

The workability, compressive strength and pore structure of the designed paste mixtures (Table 4) were analyzed. Mercury intrusion porosimetry (MIP) was used to evaluate the effect of using

admixture on the pore structure development. The paste mixtures have the same L/B ratio (0.32) and 3M NaOH alkalinity as the concrete mixtures; the admixture content per kg binder was identical with that of the tested concrete mixtures A, B, D and F with a corresponding admixture contents of 0/ 1/ 3/ 5 kg/m^3. During the sample preparation, all components were mixed at once with a Hobart mixer for 5 min at medium speed. The specimens for strength testing were prepared in polystyrene prism molds (40 × 40 × 160 mm^3), compacted on a vibration table and sealed with plastic foil. For the porosity experiments, fresh paste was cast in plastic containers (≈ 300 ml) and filled to the top and slightly tamped for air release. Sealed containers were placed on a slowly rotating apparatus to avoid particle segregation, and the rotation apparatus was stopped after paste setting after about 4 hours. Samples were stored for curing in a climate room (20 °C and ≥ 95% RH) until testing.

Table 4: Mixture composition of AAM pastes for porosity experiments.

Mixture	MB (g)	Total liquid (ml)	L/B ratio	NaOH (M)	Admixture (g/kg)	Related concrete mixture design
P0	1000	320	0.32	3	0.0	A
P1	1000	320	0.32	3	2.5	B
P3	1000	320	0.32	3	7.5	D
P5	1000	320	0.32	3	12.5	F

Admixture content in the paste mixture is multiplied by a factor 2.5, to correspond with the admixture content of the concrete mixtures A, B, D and F (Table 3), gaining equal admixture dosage per kg of binder.

2.4 Test methods

The slump of the fresh concrete was measured in accordance with NEN-EN 12350-2. During the test period, fresh concrete was mixed at very low rotation speed (imitation of real-life concrete truck transport mixer process). The flowability of the paste mixtures was determined using a Hägermann cone (100 mm base diameter, 70 mm top diameter and height 60 mm), in accordance with EN 459-2.

The compressive strength of concrete was measured at the age of 1, 7, 28 and 56 days respectively in accordance with NEN-EN 12390-3 and the strength of paste samples were performed in accordance with NEN-EN 196-1.

The material electrical resistivity was tested at the age of 28 and 91 days respectively on cubic samples (150 × 150 × 150 mm^3). The applied method was in accordance with the Two Electrodes Method (TEM) which is described in the reference [29].

The Rapid Chloride Migration (RCM) coefficient of concrete at the age of 28 and 91 days respectively was determined in accordance with the NT Build 492. Samples (150 × 150 × 150 mm^3) were stored until 24 hours after casting in a 20°C water bath, securing maximal water saturation as normally AAM concrete is preferably not cured in a water bath. The experiments were performed on fourfold drilled samples (Ø 100 mm).

The porosity measurements were performed with MIP on paste mixtures, measuring the pore sizes from 0.006 to 350 µm (twofold measurement per sample). The sample preparation procedure was the following: at different ages of 7, 28 and 56 days samples were crushed and the reaction was stopped with liquid nitrogen and then the samples were vacuum freeze dried at -28 °C, until constant mass to allow the pore solution to be removed by sublimation of ice microcrystals and maintaining the microstructure without significant damages. Mercury intrusion started at a low pressure of 0-0.003 MPa followed by a pressure increase from 0.0036 to 210 MPa. The extrusion process started immediately afterwards, during which the pressure decreased from 210 to 0.14 MPa. The surface tension and the contact angle were fixed at 0.485 N/m and 132 degrees, respectively.

3 Results and Discussions

3.1 Effect of admixture on the concrete characteristics

3.1.1 Effect of admixture on the fresh concrete workability

Figure 1 shows the fresh concrete slump over time as a function of the admixture content (0 to 5 kg/m^3) for concrete mixtures A-F, presented in Table 3. The results clearly show a significantly affected slump behavior over time, from a very stiff consistency (concrete consistency class S0) without admixture, to a more fluid and then a highly fluid consistency at higher admixture contents. At a higher admixture content of more than 4 - 5 kg/m^3, deformation mechanisms (i.e. segregation and bleeding) of the fresh concrete mixtures were observed. For the tested mixtures, 3 kg/m^3 of admixture is identified as the optimum dosage, corresponding with 0.75 wt. % of the binder content.

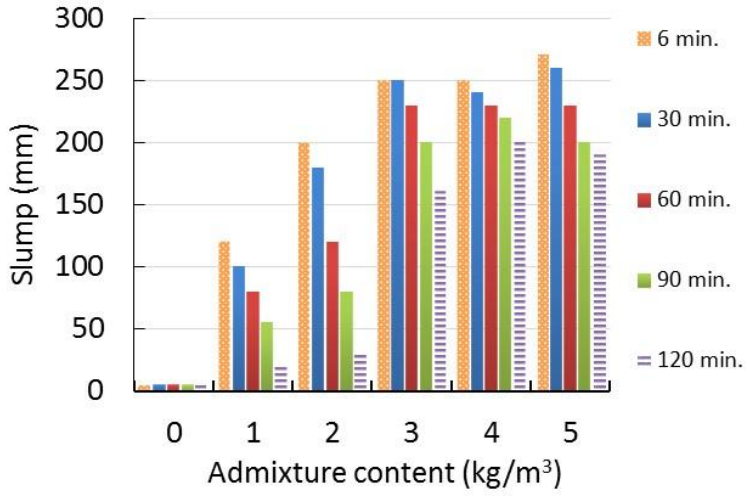

Figure 1: Slump of fresh concrete mixtures A-F between 6 to 120 min versus admixture content.

Further, the admixture was able to control the fresh concrete workability over time, showing a slowly declining slump (6 to 120 min). The slump modification by the admixture is also observed in the previous study [30], applying the same admixture in the production of ultra-

lightweight AAM concrete. However, using the admixture with a dosage of ≥ 3 kg/m^3, the retention of the slump between 6 to 120 min is clearly observed, implying an extended mixture setting time. This highly effective admixture-related result has been mainly observed in the literature for Portland cement systems [11,12,31], as admixture use in AAM systems to modify the fresh mixture workability is much less effective [15,18,32]. This can be explained by the increasing admixture adsorption behavior, as a function of a higher admixture content, onto the positively charged mineral precursor particle surfaces [12,33,34]. This connection keeps the particles sterically at distance enhancing the mixture workability which results in a delay of the microstructure development indicated by a delayed mixture setting (Figure 1) and consequently inhibited early age compressive strength progression (Figure 2) [35,36].

3.1.2 Effect of admixture on the compressive strength

Figure 2 shows the concrete compressive strength development as a function of the admixture content (0 to 5 kg/m^3), for mixtures A to F. The results indicate that a higher admixture content retards the early age (1 day) strength development. However at the age of 7 days, all admixture containing concretes exhibit ≈ 20 MPa (varying between 18 to 23 MPa), which is higher than the non-admixture reference of 15 MPa. Over time, this effect is even more significant, as the strengths increase more (42-46 MPa at 28 days) in comparison with the reference concrete (20 MPa at 28 days). It should be noted that the lower strength development from the reference concrete (containing no admixture) is attributed to the compaction influence due to its relatively stiff fresh mixture consistency (Figure 1). As no significant differences of the visible surface smoothness and measured fresh concrete material density between all tested samples is observed.

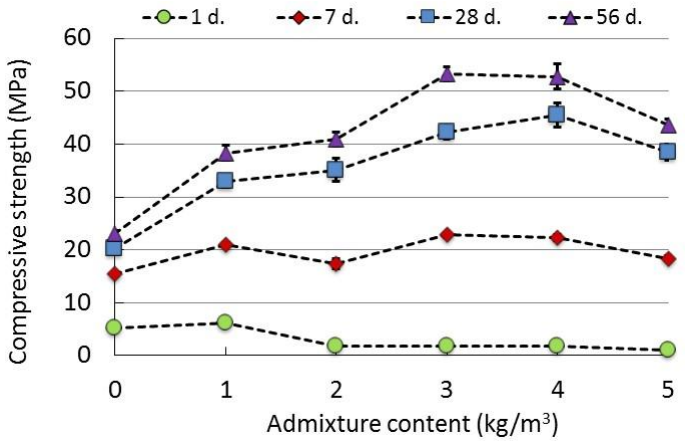

Figure 2: Compressive strength development of concretes with varying admixture contents for mixtures A-F. Error bar: deviation of the strength based on 3 concrete samples.

The optimal admixture content with regard to compressive strength is about 3 to 4 kg/m^3. The decline in strength with the admixture content of ≈ 5 kg/m^3 could be explained by the observed mixture segregation, while unstable and inhomogeneous mixtures can result in a higher concrete porosity and therefore lower strengths. This will be further discussed in Section 3.2.4. The use of admixtures, within an optimal range, improves the mixture workability and particle packing and therefore the concrete densification which consequently leads to an enhanced material strength [37]. However, apart from this, other fundamental physical and chemical admixture-related mechanisms could also be of influence:

- For the early age strength (1 to 7 days): It is known from the literature that a higher (polycarboxylate) admixture content increases and partially controls the precursor element release (mainly calcium) by slowing down the mineral precursor dissolution processes of mainly GGBS [38]. This is initiated by admixture adsorption, due to calcium bridging onto mineral surfaces and element complexation of the admixture (ligand formation) that disrupt nucleation and early age polycondensation. Further, the observed 1 day strength retardation is in line with the prolonged setting time of the fresh concrete, which is increasingly noticeable at higher admixture contents (Figure 1).
- For the later age strength (7 to 56 days): It was observed in previous research [39] that the reaction product (gel layer thickness) around GGBS particles within a 28 hardening period, is

significantly thicker with admixture compared to a non-admixture reference paste mixture, as shown in Figures 3a and 3b. This effect has been reported in the literature, on both AAM [14] and Portland cement [26] systems with the enhanced matrix development, by densifying the interfacial transition zone (ITZ) between: (I) the newly formed gel matrix and solid-binder and (II) the newly formed gel matrix and the aggregate particles [26], which can lead towards a modified material strength performance (Figure 2). This will be further discussed in sections 3.2.3 and 3.2.4.

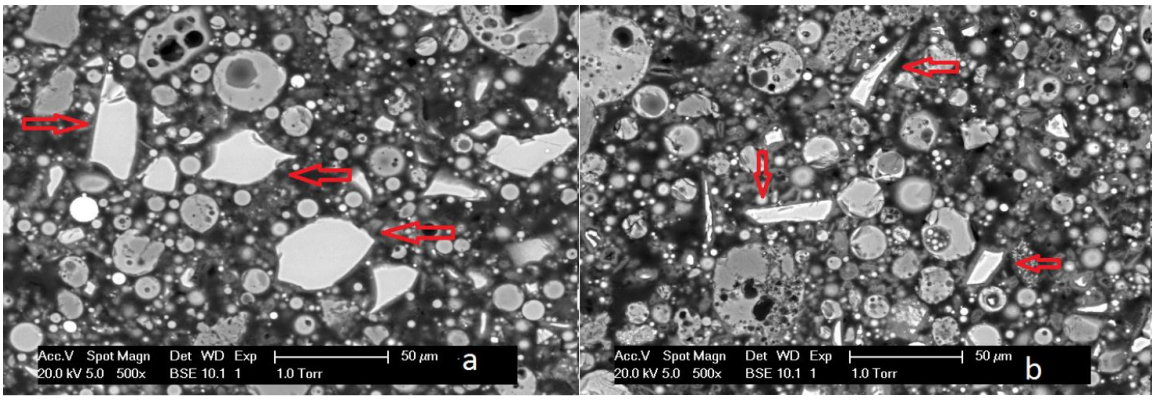

Figure 3: Environmental scanning electron microscopy (ESEM) pictures of gel layer thickness around PCFA and GGBS particles within paste samples at 28 days of age of (a) paste without admixture and (b) with admixture (paste mixture comparable with P3). The GGBS particles (red arrow) are overall light grey, rectangular shaped, while PCFA are darker grey, round shaped containing hollow spheres

3.1.3 Effect of admixture on the Cl-migration

The previous sections demonstrated that the admixture content strongly influences the fresh and hardened state AAM concrete performance over time. Figures 4a and 4b show the effect of the admixture content (0 to 5 kg/m^3) on the Cl-migration coefficient (abbreviation is Drcm) of concrete mixtures A to F, at the age of 28 and 91 days, respectively. At the age of 28 days, the Cl-migration rate in concrete is strongly influenced by the admixture content, as shown in Figure 4a. Samples containing 0-2 to about 3 kg/m^3 admixture have a comparable and low (approximately 3 × 10^{-12} m^2/s) Cl-migration, even though, the initial fresh mixture slump increases significantly as an effect of a higher admixture dosage (Figure 1). Additionally, this indicates that the references sample (containing no admixture) possess a high compaction level and related matrix density even though its relative stiff fresh mixture consistency.

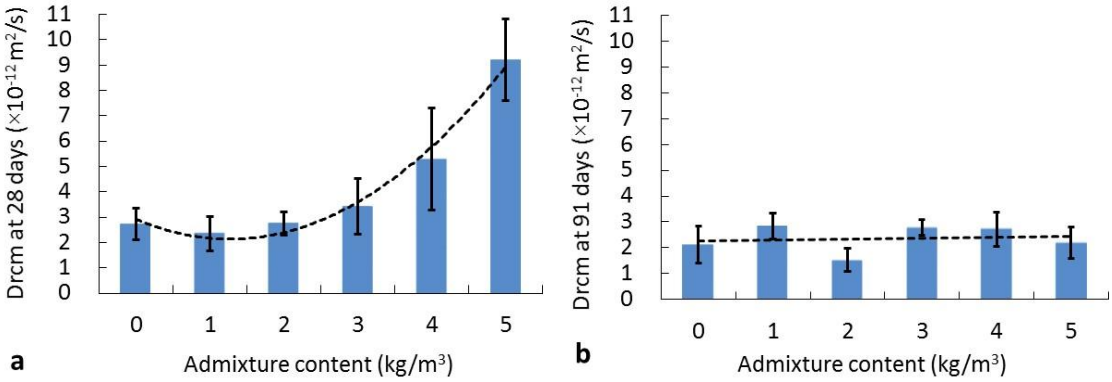

Figure 4: Chloride migration coefficient of (a) 28 and (b) 91 days old AAM concretes with varying admixture contents for mixtures A-F. The dashed line is the trend line.

The overall performance (mixtures containing 0-2 to about 3 kg/m^3 admixture) is in line with the literature [9], stating that AAM and specifically fly ash-dominated systems can obtain a low Cl-diffusion rate. On the contrary, at a high admixture content of ≥ 3 - 5 kg/m^3, the Cl-migration coefficient strongly increases at which these three D_{rcm} values are followed by a perfect exponential trend (R: 1.00). This increase, is probably related to a higher porosity or abundance of capillary pores caused by the segregation, consequently higher permeability of the concrete that strongly influences the Cl-migration [9]. This effect can also be compared with a higher liquid content or higher L/B ratio, which also significantly increases the porosity [40]. The AAM porosity properties is further discussed in Section 3.2.3, in addition further study is needed to gain more understanding of the observed results. For the 91 days results (Figure 4b), all concrete mixtures (non- to high admixture contents) show a decrease in Cl-migration, towards a comparable and low level of about 2.6 × 10^{-12} m^2/s. Surprisingly, mixtures with an admixture content ≥ 3 kg/m^3 show the most significant Cl migration coefficient decline. This effect can be assumed to be controlled by the element dissolution behavior of PCFA in the binder, favoring a further densification of the matrix [9,41] and consequently improved strength (Figure 2), resulting in a reduced diffusion rate. This effect is also observed in the literature [42–45], showing that the matrix of AAM and Portland cement based mixture, containing PCFA, significantly densifies in the period of 28 to 91 days after casting. Additionally, material electrical resistivity served in this study as a quick and reliable indicator to determine the

concrete permeability and related Cl-migration performance [29]. Figure 5 shows the Cl-migration coefficient in relation with the material electrical resistivity of 28 and 91 days old AAM concrete mixtures A to F.

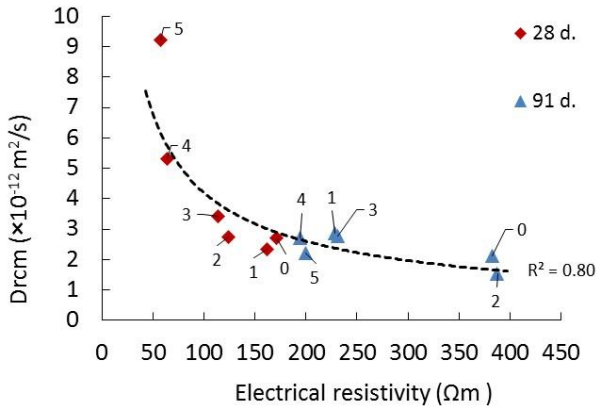

Figure 5: The relation between Cl-migration rate (Drcm) and material electrical resistivity of AAM concretes at 28 and 91 days for mixtures A-F. The numbers close to data points are the admixture content (g/kg). All samples' pH range between 12.0 to 12.5.

The results show a significant resistivity increase when increasing the concrete age from 28 to 91 days, as well as a decreased Drcm over time. This behavior is comparable with Portland slag cement mixtures [29], although overall the AAM concrete mixtures exhibit far lower resistivity values. in comparison, at 28 days the Portland cement mixtures show RCM values ranging between about 1 - 5 × 10^{-12} m^2/s with an electrical resistivity ranging between 175 - 500 Ωm [29], where the representative AAM value range between about 2 -5 × 10^{-12} m^2/s with a resistivity ranging between 60 - 175 Ωm. This difference in resistivity between both systems is maintained when the age of the concrete increases. Further, the electrical resistivity of both systems strongly increase, which is an indication of further material densification and consequently lower permeability. The Cl-migration and electrical resistivity results also indicate that the effect of the admixture content is related to the porosity development of paste and accordingly of concrete samples (further discussed in Section 3.3).

3.2 Effect of admixture on the paste characteristics

3.2.1 Effect of admixture on the fresh paste flowability

The paste slump was measured directly after mixing and showed a similar behavior (flowability modifying effect) as observed in the concrete mixtures (Figure 1). An increase of paste flowability as a function of admixture content: 0/ 1/ 3/ 5 g/kg admixture resulted in a slump of 200/ 230/ 240/ 250 mm, respectively (obtained data points follow a logarithmic trend (R: 0.95)).

3.2.2 Effect of admixture on the compressive strength

Figure 6 plots the compressive strength development of paste as a function of the admixture content (0 to 5 g/kg binder) for mixtures P0 to P5, which are described in Table 4. A higher admixture content slightly retards the early age strength development. While at 28 days, the strength is increased when increasing the admixture content. The admixture related strength development shows strong similarities with that of the tested concrete mixtures, as described in Section 3.1.2. Additionally, the paste slump, measured directly after mixing, shows a similar behavior (flowability modifying effect) observed for the concrete mixtures due to the increase of the flowability at an increased admixture dosage. It should be noted that difference in strength increase in paste and concrete is obverted, which might be attributed to several reasons, including aggregate type and content, workability, compaction effort and particle packing.

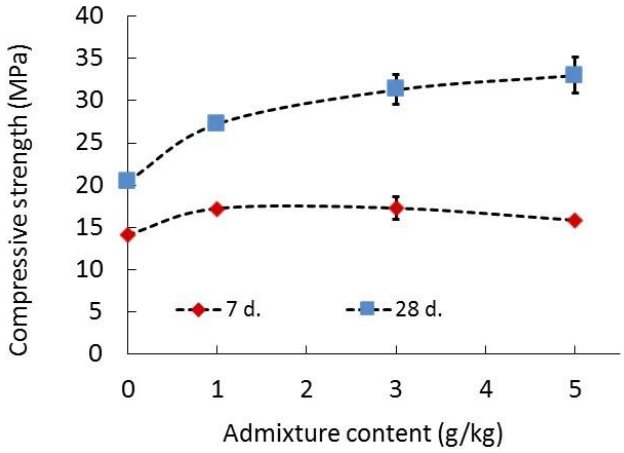

Figure 6: Compressive strength development of AAM paste mixtures P0-P5 versus admixture content.

3.2.3 Effect of admixture on the porosity

Figures 7-9 show the development of the AAM paste porosity (7 to 56 days) of medium to large pore size (0.01 to 100 µm), as a function of the admixture content (0 to 5 g/kg binder) for mixtures P0 to P5. It is shown in Figure 7 that after 7 days AAM pastes with 0 and 1 g/kg admixture have a similar size pore distribution. However, at high admixture contents (3 to 5 g/kg), larger pores are observed in the paste mixtures, which is shown (Figure 7b) by an extreme growth (hump) for 1-2 µm pores. At the age of 28 to 56 days, this hump completely disappears for all samples, only pores with smaller size or a refined porosity are observed, as shown in Figures 8 and 9. The results also show a more refined paste pore structure as a function of the increasing admixture content.

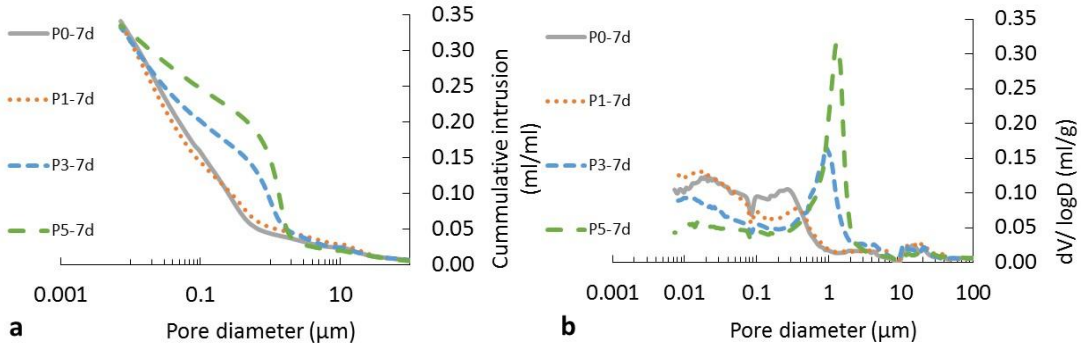

Figure 7: Pore size distribution at 7 days of age of AAM paste for mixtures P0-P5, with a varying admixture content: (a) pore size distribution; (b) pore size distribution differential curve.

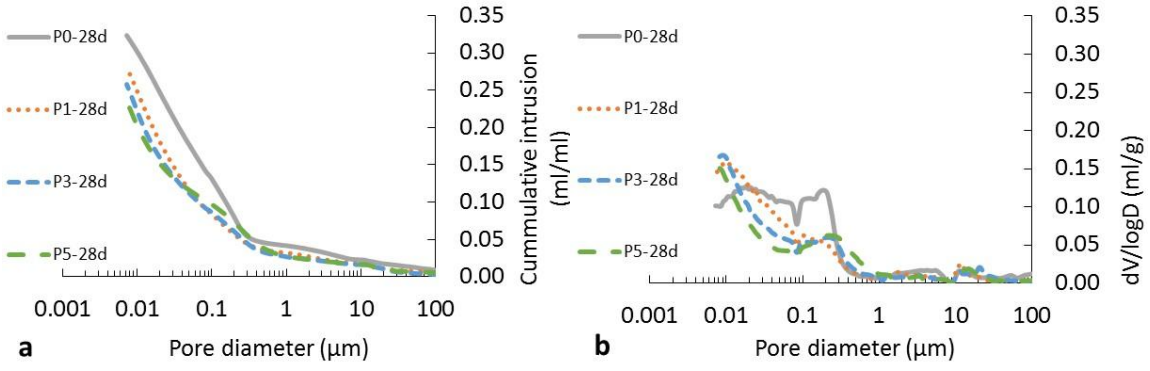

Figure 8: Pore size distribution at 28 days of age of AAM paste mixtures P0-P5 with varying admixture content: (a) pore size distribution; (b) pore size distribution differential curve.

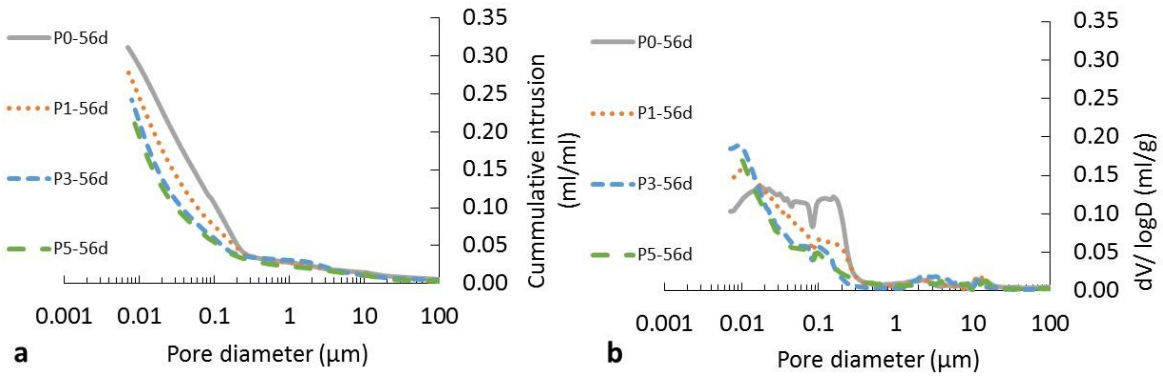

Figure 9: Pore size distribution at 56 days of age of AAM paste mixtures P0-P5 with varying admixture contents: (a) pore size distribution; (b) pore size distribution differential curve.

Two distinct pore types are identified as being critical with regard to material strength and liquid and ion transport for paste or concrete: (1) effective capillary pores that vary between 0.01 to 10 µm (10 to 10.000 nm) and (2) gel pores with a size < 0.01 µm (< 10 nm) [46,47]. Figures 10a and 10b show the total and effective capillary porosity development (7 to 56 days) of AAM pastes, as a function of the admixture content (0 to 5 g/kg binder) for mixtures P0 to P5.

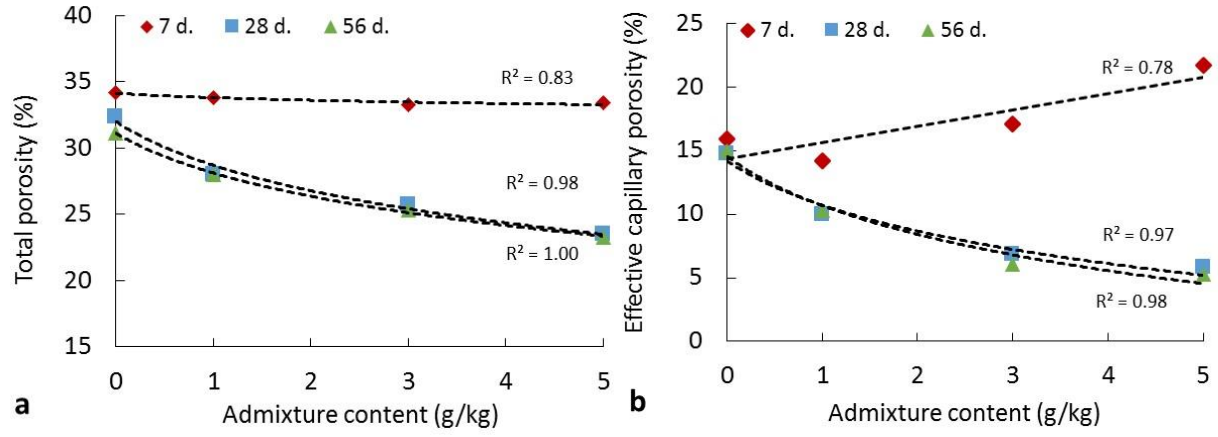

Figure 10: Porosity development at 7/ 28/ 56 days of age of AAM paste mixtures P0-P5 with varying admixture contents: (a) Total porosity; (b) Effective capillary porosity.

With regard to the total porosity (Figure 10a), all samples show similar values after 7 days of curing. However, over time after 28 and 56 days, the total porosity is significantly decreased at an increasing admixture content, following a logarithmic trend. The measured porosity of the non-admixture containing reference mixture (P0) is in line with the literature [7]. A different behavior is observed for the effective capillary porosity (Figure 10b). At 7 days, an increase in effective capillary porosity is related to a higher admixture content (followed by a linear trend). However, further over time at 28 to 56 days, this effect is altered, where a lower effective capillary porosity is obtained at an increasing admixture content (followed by a logarithmic trend). This admixture effect of pore structure refinement in AAM has never been reported in the literature. Often a reduced porosity over time in AAM is observed , when a higher GGBS binder content instead of PCFA and or alkaline activator (silicate source) is used [41]. In addition, Figure 11 shows the relation between the total porosity and the effective capillary porosity dependent on the admixture content over time for AAM pastes (original data of Figs 10a, b). The results show a strong decrease of the total porosity at a decreasing effective capillary porosity over time with a higher admixture content, following a logarithmic trend.

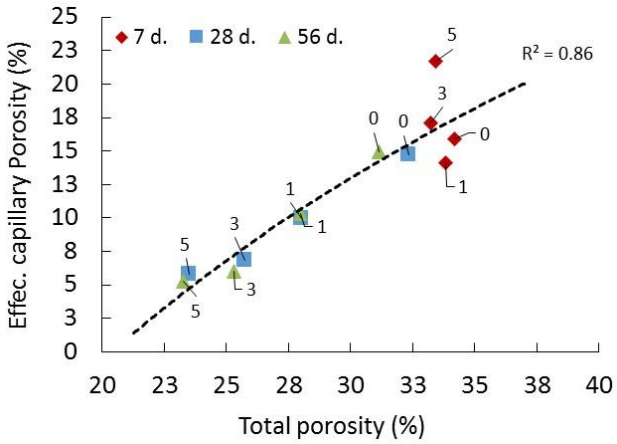

Figure 11: Correlation between total and effective capillary porosity at 7, 28 and 56 days of age for AAM paste for mixtures P0-P5. Values close to the data points are the admixture content (g/kg).

3.2.4 Porosity versus strength progression

Figure 12 shows the relation and prediction (trend) between the total and effective capillary paste porosity and the paste compressive strengths over time. Firstly, a higher admixture content results in a lower total and effective capillary porosity over time at the age of 28 days

and therefore increases the material strength. Secondly, the relation between strength and porosity of cement-based (porous) materials such as AAM can be predicted by using a (non)-linear trend. As a linear trend sometimes overestimates the results and the literature [48] indicates that both porosity parameters follow a different trend to explain the strength. For the total porosity, a linear trend is used and for the effective capillary porosity a logarithmic trend is derived. Both findings are in line with the literature on Portland cement mortars [48].

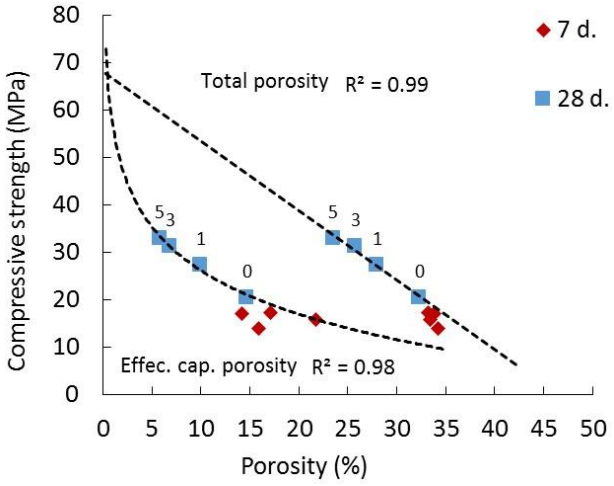

Figure 12: Correlations between: paste compressive strength and the total and effective capillary paste porosities over time (7 to 28 days age) for mixtures P0-P5. Values close the 28 days data points are the admixture contents (g/kg). Fitted lines are based on data point at 28 days of age.

3.3 AAM concrete discussions

The results presented in the previous sections on paste and concrete mixtures show that the use of a plasticizing admixture enhances the flowability properties and the hardened state performance of AAM. Figure 13 shows the relation between the Cl-migration coefficient (Drcm) at 28 days of AAM concretes and the total and effective capillary porosity of AAM pastes at 28 days. From this correlation it can be concluded that AAM concretes with a low to optimal admixture content (1 to 3 kg/m^3) possesses a low Cl-migration rate and related material electrical resistivity as shown in Figure 5, indicating a low permeability. This is in line with the significant pore structure refinement over time as shown in Figures 7 to 9. This refinement is significantly enhanced by admixture with a proper dosage, as the ingress of Cl-ions is largely controlled by the concrete permeability which is influenced by the porosity while excessive

admixture amount leads to segregation and higher porosity [41,43,44]. Furthermore, this AAM matrix densification effect by using admixture is supported by the literature on Portland cement mixtures [37], and this effect is observed and detailed analyzed in the previous study [39] of AAM paste mixtures, as shown in Figure 3. Where scanning electron microscopy (SEM) analysis showed that the matrix of a AAM paste, at 28 days age (containing about 3 kg/m^3 of admixture, which is found to be the optimal content in the present study), has a significantly thicker (≈ 34%) newly formed gel layer around the GGBS particles instead of the non-admixture reference samples. This leads to a more densified and lower permeable AAM matrix with a significantly higher compressive strength (supported by Figure 2), which is strongly related to a lower total porosity as supported by Figure 12.

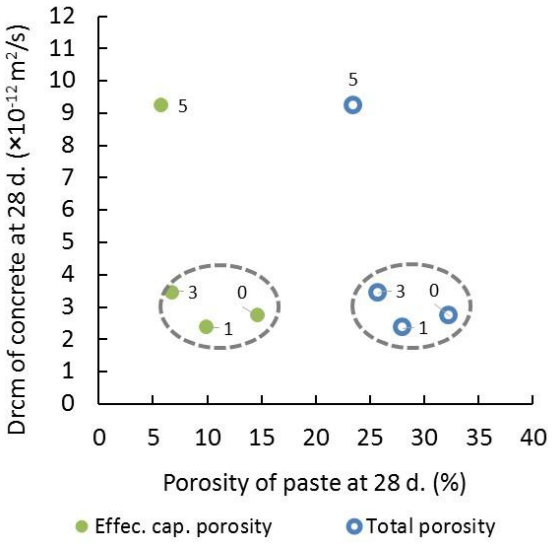

Figure 13: Chloride migration of 28 days old AAM concretes (mixtures A/B/D/F of Table 3) in relation to the total and effective capillary porosity of 28 days old AAM pastes (mixtures P0-P5). Values close to the data points are the admixture contents (g/kg in paste and kg/m^3 in concrete).

The plotted data in Figure 13 show that both the total and effective paste porosity within a defined range have comparable influences on the Cl-migration in concrete. No distinct trend can be observed between both porosity parameters and their individual influences on Cl-migration, which can be explained by the fact that both parameters at 28 days age are strongly related with each other (Figure 11). However, data obtained from a preliminary study [49] on a 28-day old admixture-modified AAM concrete (mixture comparable with AAM mixture D using

469 3 kg/m^3 of admixture), show a relatively high abundance of connected spherical voids in the
470 matrix. This is supported by the literature [43,47], reporting that the matrix permeability of
471 PCFA-dominated AAM and Portland cement pastes is strongly related with the effective
472 capillary porosity. Since the connected pores provide a continuous channel for transport, they
473 largely affect the permeability and the ion ingress in the matrix [43,44]. It should be noted that
474 the porosities shown in Figure 13 were acquired from paste sample while the Cl-migration
475 results were based on concrete samples. As mentioned in Section 3.1.1, a higher admixture
476 dosage than 3 kg/m^3 results in concrete segregation that leads to a clearly increased Cl-
477 migration (mix 5 in Figure 13). Nevertheless, it can be concluded that both total porosity and
478 effective capillary porosity can be used to indicate the Cl-migration property in AAM.
479

4 Conclusions

The effects of a polycarboxylate admixture on the flowability properties and hardened state performance of AAM concrete and paste mixtures are investigated. The relations between the alteration of the pore structure and related material strength and chloride ingress that are changed, dependent on the admixture content, are evaluated. Based on the obtained results, the following conclusions can be drawn:

- The workability of the fresh AAM concrete significantly improves from a zero slump towards a maximal measurable slump value (> 250 mm) with a relatively low admixture content (0.25-0.75 wt.% of the binder). At which it is likely that the setting time of the concrete mixture is increasingly prolonged with a higher admixture content, even up to 120 min at an admixture content of about 3 kg/m^3.
- The concrete compressive strength progresses significantly over time at higher admixture contents. The 7 and 28 days compressive strength of admixture-containing concrete (at an optimal admixture content (3 to 4 kg/m^3)) are about 22 and 44 MPa, respectively, while that of the reference concrete are only 15 and 23 MPa, respectively.
- The pore structure of the AAM paste mixtures is strongly refined over time at an increasing admixture content, resulting in a significant decrease of the total and effective capillary porosity and reduced material permeability. A significant relation is found between the compressive strength and the porosity.
- The chloride migration coefficients of admixture-modified AAM concrete at the age of 28 and 91 days, at an optimal admixture content, are about 3.0×10^{-12} m^2/s and 2.6×10^{-12} m^2/s, respectively. A relation between the Cl-migration coefficient (Drcm) and material electrical resistivity (Ωm) over time is derived for the AAM concrete mixtures.

Acknowledgements

The authors thank their research sponsors Van Gansewinkel Minerals, Cementbouw Mineralen and SQAPE Technology, all from the Netherlands. We wish to express our gratitude to Mr. D. Duprie and Mr. G. van der Berg and Dr. P.I.J. Kakebeeke, all from Cementbouw, for their laboratory support and expert judgement on the concrete production.

References

1. Arbi, K., Nedeljković, M., Zuo, Y. & Ye, G. A Review on the Durability of Alkali-Activated Fly Ash/Slag Systems: Advances, Issues, and Perspectives. *Industrial & Engineering Chemistry Research* (2016). doi:10.1021/acs.iecr.6b00559

2. Provis, J. L. & Bernal, S. A. Geopolymers and Related Alkali-Activated Materials. *Annual Review of Materials Research* **44,** 299–327 (2014).

3. *Handbook of Alkali-activated cement, mortars and concretes*. (Woodhead Publishing, 2015).

4. *Alkali Activated Materials, state of the art report, RILEM TC 224-AAM*. **13,** (Springer, 2014).

5. Deb, P. S., Nath, P. & Sarker, P. K. The effects of ground granulated blast-furnace slag blending with fly ash and activator content on the workability and strength properties of geopolymer concrete cured at ambient temperature. *Materials & Design* **62,** 32–39 (2014).

6. Ismail, I. *et al.* Modification of phase evolution in alkali-activated blast furnace slag by the incorporation of fly ash. *Cement and Concrete Composites* **45,** 125–135 (2014).

7. Lee, N. K., Jang, J. G. & Lee, H. K. Shrinkage characteristics of alkali-activated fly ash/slag paste and mortar at early ages. *Cement and Concrete Composites* **53,** 239–248 (2014).

8. Gao, X., Yu, Q. L. & Brouwers, H. J. H. Reaction kinetics, gel character and strength of ambient temperature cured alkali activated slag–fly ash blends. *Construction and Building Materials* **80,** 105–115 (2015).

9. Ismail, I. *et al.* Influence of fly ash on the water and chloride permeability of alkali-activated slag mortars and concretes. *Construction and Building Materials* **48,** 1187–1201 (2013).

10. Huang, H. *et al.* Improvement on microstructure of concrete by polycarboxylate superplasticizer (PCE) and its influence on durability of concrete. *Construction and*

Building Materials **110,** 293–299 (2016).

11. *Science Technology of concrete admixtures*. (Woodhead Publishing, 2016).

12. Flatt, R. J. Superplasticizers and the rheology of concrete. in *Understanding the rheology of concrete* (ed. Roussel, N.) 144–201 (Woodhead Publishing, 2012).

13. Nematollahi, B. & Sanjayan, J. Effect of different superplasticizers and activator combinations on workability and strength of fly ash based geopolymer. *Materials and Design* **57,** 667–672 (2014).

14. Demie, S., Nuruddin, M. F. & Shafiq, N. Effects of micro-structure characteristics of interfacial transition zone on the compressive strength of self-compacting geopolymer concrete. *Construction and Building Materials* **41,** 91–98 (2013).

15. Rashad, A. M. A comprehensive overview about the influence of different admixtures and additives on the properties of alkali-activated fly ash. *Materials & Design* **53,** 1005–1025 (2014).

16. Arbi, K. *et al.* Experimental study on workability of alkali activated fly ash and slag-based geopolymer concretes. in *Geopolymers: The route to eliminate waste and emissions in ceramic and cement manufacturing. ISBN: 9781326377328* 75–78 (ECI, 2015).

17. Aliabdo, A. A., Abd Elmoaty, A. E. M. & Salem, H. A. Effect of water addition, plasticizer and alkaline solution constitution on fly ash based geopolymer concrete performance. *Construction and Building Materials* **121,** 694–703 (2016).

18. Jang, J. G., Lee, N. K. & Lee, H. K. Fresh and hardened properties of alkali-activated fly ash/slag pastes with superplasticizers. *Construction and Building Materials* **50,** 169–176 (2014).

19. Rashad, A. M. Alkali-activated metakaolin: A short guide for civil Engineer – An overview. *Construction and Building Materials* **41,** 751–765 (2013).

20. Rashad, A. M. A comprehensive overview about the influence of different additives on the properties of alkali-activated slag – A guide for Civil Engineer. *Construction and*

Building Materials **47,** 29–55 (2013).

21. Al-Majidi, M., Lampropoulos, A. & Cundy, A. Effect of Alkaline Activator , Water , Superplasticiser and Slag Contents on the Compressive Strength and Workability of Slag-Fly Ash Based Geopolymer Mortar Cured under Ambient Temperature. *International Journal Civil, Environmental ---- Architectural Engineering* **10,** 285–289 (2016).

22. Puertas, F., Palacios, M. & Provis, J. L. Admixtures. in *Alkali activated materials, State-of-the-art report, RILEM TC 224-AAM* (eds. Provis, J. L. & van Deventer, J. S. J.) 145–156 (Springer, 2014).

23. Nematollahi, B. & Sanjayan, J. Efficacy of available superplasticizers on geopolymers. *Research Journal of Applied Sciences, Engineering and Technology* **7,** 1464–1468 (2014).

24. Bilim, C., Karahan, O., Atiş, C. D. & İlkentapar, S. Influence of admixtures on the properties of alkali-activated slag mortars subjected to different curing conditions. *Materials & Design* **44,** 540–547 (2013).

25. Palacios, M., Houst, Y. F., Bowen, P. & Puertas, F. Adsorption of superplasticizer admixtures on alkali-activated slag pastes. *Cement and Concrete Research* **39,** 670–677 (2009).

26. Hu, J. Porosity of Concrete - Morphological Study of Model Concrete. (Delft Univerity of Technology, 2004).

27. Komnitsas, K. & Zaharaki, D. Utilisation of low-calcium slags to improve the strength and durability of geopolymers. in *Geopolymers. Structure, processing, properties and industrial applications.* (eds. Provis, J. L. & Deventer, J. S. J. Van) 343–375 (Woodhead Publications, 2009).

28. Hunger, M. & Brouwers, H. J. H. Flow analysis of water–powder mixtures: Application to specific surface area and shape factor. *Cement and Concrete Composites* **31,** 39–59 (2009).

29. Van Noort, R., Hunger, M. & Spiesz, P. Long-term chloride migration coefficient in slag

592 cement-based concrete and resistivity as an alternative test method. *Construction and*
593 *Building Materials* **115,** 746–759 (2016).

594 30. Huiskes, D. M. A., Keulen, A., Yu, Q. L. & Brouwers, H. J. H. Design and performance
595 evaluation of ultra-lightweight geopolymer concrete. *Materials & Design* **89,** 516–526
596 (2015).

597 31. Houst, Y. F. *et al.* Design and function of novel superplasticizers for more durable high
598 performance concrete (superplast project). *Cement and Concrete Research* **38,** 1197–
599 1209 (2008).

600 32. Rashad, a. M., Bai, Y., Basheer, P. a. M., Milestone, N. B. & Collier, N. C. Hydration and
601 properties of sodium sulfate activated slag. *Cement and Concrete Composites* **37,** 20–29
602 (2013).

603 33. Ferrari, L., Kaufmann, J., Winnefeld, F. & Plank, J. Interaction of cement model systems
604 with superplasticizers investigated by atomic force microscopy, zeta potential, and
605 adsorption measurements. *Journal of colloid and interface science* **347,** 15–24 (2010).

606 34. Habbaba, A. & Plank, J. Interaction Between Polycarboxylate Superplasticizers and
607 Amorphous Ground Granulated Blast Furnace Slag. *Journal American Ceramic Society*
608 **2863,** 2857–2863 (2010).

609 35. Gelardi, G. & Flatt, R. J. Working mechanisms of water reducers and superplasticizers. in
610 *Science and Technology of Concrete Admixtures* (eds. Aïtcin, P.-C. & Flatt, R. J.) 527–275
611 (Woodhead Publishing, 2016).

612 36. Marchon, D. & Flatt, R. J. Impact of chemical admixtures on cement hydration. in *Science*
613 *and Technology of Concrete Admixtures* (eds. Aïtcin, P.-C. & Flatt, R. J.) 279–299
614 (Woodhead Publishing, 2016).

615 37. Toledano-Prados, M., Lorenzo-Pesqueira, M., González-Fonteboa, B. & Seara-Paz, S.
616 Effect of polycarboxylate superplasticizers on large amounts of fly ash cements.
617 *Construction and Building Materials* **48,** 628–635 (2013).

618 38. Suraneni, P., Palacios, M. & Flatt, R. J. New insights into the hydration of slag in alkaline
619 media using a micro-reactor approach. *Cement and Concrete Research* **79,** 209–2016
620 (2015).

621 39. Zhang, S. Analytical elements identification of geopolymer paste on network structure
622 influenced by different specific geopolymer admixtures. (Delft Univerity of Technology,
623 2014).

624 40. Chen, X. & Wu, S. Influence of water-to-cement ratio and curing period on pore structure
625 of cement mortar. *Construction and Building Materials* **38,** 804–812 (2013).

626 41. Zhang, Z. & Wang, H. Analysing the relation between pore structure and permeability of
627 alkali-activated concrete binders. in *Handbook of Alkali Activated Cements, Mortars and*
628 *Concretes* (eds. Pacheco-Torgal, F., Labrincha, J. A., Leonelli, C., Palomo, A. &
629 Chindaprasirt, P.) 235–262 (Woodhead Publications, 2015).

630 42. Siddique, R. & Khan, M, I. Fly ash. in *Supplementary cementing materials* 1–61 (Springer,
631 2011).

632 43. Yu, Z. Microstructure Development and Transport Properties of Portland Cement-fly Ash
633 Binary Systems. (Technical University Delft, 2015).

634 44. Ma, Y., Hu, J. & Ye, G. The pore structure and permeability of alkali activated fly ash. *Fuel*
635 **104,** 771–780 (2013).

636 45. Liu, J., Wang, X., Qiu, Q., Ou, G. & Xing, F. Understanding the effect of curing age on the
637 chloride resistance of fly ash blended concrete by rapid chloride migration test. *Materials*
638 *Chemistry and Physics* **196,** 315–323 (2017).

639 46. Cook, R. A. & Hover, K. C. Mercury porosimetry of hardened cement pastes. *Cement and*
640 *concrete research* **29,** 933–943 (1999).

641 47. Ma, Y. Microstructure and Engineering Properties of Alkali Activated Fly Ash -as an
642 environment friendly alternative to Portland cement. (Delft Technical University of
643 Technology, 2013).

644 48. Chen, X., Wu, S. & Zhou, J. Influence of porosity on compressive and tensile strength of
645 cement mortar. *Construction and Building Materials* **40,** 869–874 (2013).

646 49. Valcke, S. *Durability and Microstructure, Akali activated concrete*. (2012).

647